ADVANCES IN INORGANIC CHEMISTRY, VOL. 38

ACONITASE: AN IRON–SULFUR ENZYME

MARY CLAIRE KENNEDY* and C. DAVID STOUT†

* Department of Biochemistry, Medical College of Wisconsin, Milwaukee, Wisconsin 53226
† Department of Molecular Biology, The Scripps Research Institute, La Jolla, California 92037

I. Introduction

Although the presence and function of the Krebs cycle enzyme aconitase [aconitate hydratase; citrate (isocitrate) hydro-lyase; EC 4.2.1.3] has been known for over 50 years (*1*), it is only recently that many of the unusual properties of this protein can be understood in molecular terms. The enzyme catalyzes the stereospecific conversion of citrate to threo-D_s-isocitrate via the obligatory intermediate *cis*-aconitate as illustrated in Eq. (1).

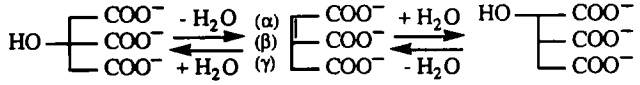

(1)

It was shown early on, particularly for the mitochondrial form of the enzyme, that activity lost during isolation could be restored upon addition of Fe^{2+} and reductant. It was only with the discovery that aconitase was an Fe–S protein (*2*) and after evidence had been obtained for the existence of 3Fe clusters (*3*, *4*) that this phenomenon could be explained. Through the application of spectroscopy, especially Möss-

bauer (MB) spectroscopy in combination with electron paramagnetic resonance (EPR), in addition to chemical methods, it was established that the activation process involved the conversion of a [3Fe–4S] cluster to a [4Fe–4S] form (Fig. 1) (*5, 6*). Furthermore, these studies demonstrated that the iron added during this reaction, labeled Fe_a, was site specific. These discoveries in the early 1980s allowed for the subsequent design of a number of experiments to investigate details of the role of the cluster in the catalytic mechanism of the enzyme (*7*). A review by Emptage discusses in some detail how knowledge of aconitase has developed through the years (*8*).

II. Properties of the Fe–S Cluster

Aconitase and ferredoxin (Fd) II of *Desulfovibrio gigas* were among the first proteins that were shown to contain a 3Fe cluster (*4*). Because of its low molecular mass and its stability, Fd II of *D. gigas* became the prime example for spectroscopic characterization of proteins containing 3Fe clusters (*9*). Many of the properties originally found in studies on Fd II were later shown to occur also in aconitase. The $1e^-$ reduced $[3Fe–4S]^0$ state of Fd II was recognized as the simplest cluster state

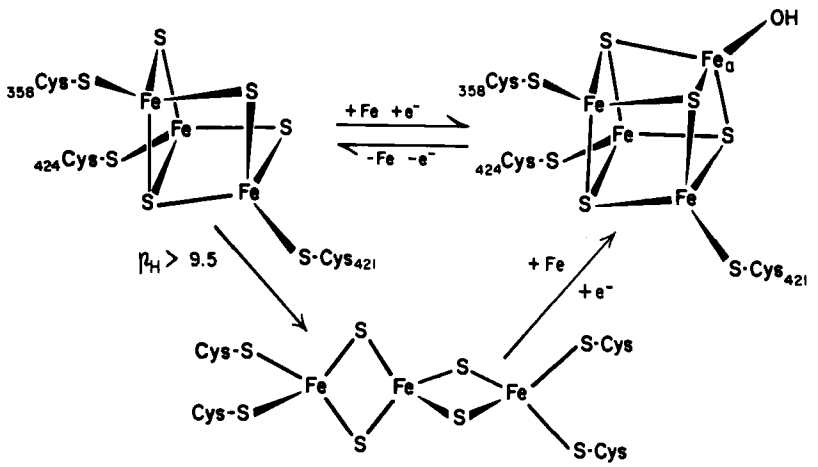

FIG. 1. Schematic description of the interconversions of the clusters in aconitase. The Cys residues bound to the linear cluster are those at positions 250, 257, 421, and 424. Their precise disposition at the cluster is not known (*26*). (Reproduced with permission from Ref. 7. Copyright 1989, Federation of European Biochemical Societies.)

that has a substructure with distinct localization of valence (*10*). Two Fe atoms share the extra electron added on reduction, and the third Fe remains ferric. The ferromagnetically coupled ($S = \frac{9}{2}$) ferric–ferrous pair containing the delocalized electron interacts antiferromagnetically with the ferric ion ($S = \frac{5}{2}$), resulting in a spin system of $S = 2$, in which the extra electron remains localized on two Fe ions. This coupling mode is thought to be due to what has become known as "double exchange" or "resonance splitting" (*10, 11*). This feature appears to be an intrinsic property of $[3Fe–4S]^0$ clusters. An analysis of this phenomenon has led to significant theoretical advances in our understanding of the electronic structure of the various Fe–S clusters. This has been considered and discussed in detail in recent literature (*10, 12, 13*). It has also been established for Fd II that the $[3Fe–4S]^0$ form is in fact not EPR silent, as previously thought (*9*), but has a broad signal at low field (<1000 G at X-band) now known to be typical of integer spin systems (*14*).

As mentioned above, the features originally described for Fd II have also been observed with aconitase, although usually at a lower signal-to-noise ratio. However, aconitase has a number of properties that make it more suitable for the detailed exploration of certain aspects. Because of the greater lability of the Fe–S cluster of aconitase, the Fe : S stoichiometry, namely 3Fe : 4S, could be determined much more convincingly for aconitase than for Fd II (*15*), and the conversion between the 3Fe and 4Fe forms could be readily followed (*6*). Because the Fe–S cluster in aconitase is more labile and because a reconstitutable apoprotein could be prepared (*16*), it was also possible to incorporate isotopes of Fe (*6*) or S (*17*) or even Se (*18*) instead of S in the cluster. This was a great advantage for spectroscopy. For aconitase it could be shown that Fe_a, the Fe that was removed by oxidation in the 4Fe → 3Fe conversion, was returned to exactly the same position from which it had been removed (*5, 6*). This position is uniquely characterized by a MB doublet of $\delta = 0.45$ and $\Delta E_Q = 0.80$ mm/sec as compared to $\delta = 0.45$ and $\Delta E_Q = 1.30$ mm/sec for the other three Fe atoms (Fe_{b1-3}) of the cluster. These unique MB features of Fe_a, along with the fact that aconitase is an enzyme whose activity can be readily determined, have been very helpful in exploring the cluster properties of aconitase.

The native form of the active enzyme contains a diamagnetic $[4Fe–4S]^{2+}$ cluster that can be reduced to the EPR-detectable $[4Fe–4S]^+$ form with the enzyme still retaining 30% activity (*19*). The EPR spectra of this latter form in the absence and presence of substrate are dramatically different, thus establishing that there is direct interaction of the substrate with the cluster. This interaction was specifically

narrowed by MB spectroscopy to the ligation of substrate to Fe_a (*20, 21*). The MB spectrum of enzyme labeled with ^{57}Fe in Fe_a gives a single doublet with the parameters given above; the spectrum changes upon addition of substrate to give two new doublets, with substantially different characteristics (*21*). These new signals, labeled S_1 and S_2, were interpreted as arising from a change in coordination of Fe_a from tetrahedral to five or six coordinate (*20, 21*). Formally, the $[4Fe–4S]^{2+}$ cluster has two Fe(III) and two Fe(II) atoms. Spectroscopy indicates that, generally in $[4Fe–4S]^{2+}$ clusters, the *d* electrons are delocalized over the whole cluster structure (*12, 22*). However, for the $[4Fe–4S]^{2+}$ cluster of aconitase, MB spectroscopy has shown that Fe_a acquires distinct ferrous character on addition of substrate to the +2 form, indicating a pronounced localization of valence at Fe_a. Electron–nuclear double-resonance spectroscopy (ENDOR) cannot give information on the diamagnetic +2 form. For the reduced $[4Fe–4S]^{+}$ cluster, however, both MB (*21*) and ENDOR (*23*) spectroscopies indicate a high degree of inequivalence among the Fe atoms, which becomes even more pronounced in the presence of substrate. The +1 cluster has formally one Fe(III) and three Fe(II). Two pairs of Fe atoms can be distinguished in the +1 cluster: a mixed-valence delocalized ferric–ferrous pair (Fe_{b2} and Fe_{b3}), and a ferrous pair (Fe_a and Fe_{b1}), where the electron added on reduction largely resides. The observation of substructures consisting of two pairs of Fe atoms is in agreement with findings on other Fe–S proteins (*24*). However, a localization of valence of the magnitude found with aconitase has previously not been seen with Fe–S proteins. These results from the MB and ENDOR spectroscopic studies on aconitase together with theoretical work (*13*) have contributed to formation of the basis for present concepts of the substructure of multinuclear Fe–S clusters and are discussed in more detail in Refs. *10, 12,* and *13*. It might be mentioned that it was possible to deduce from ^{33}S ENDOR measurements that the sulfides in the $[4Fe–4S]^{+}$ cluster, with and without substrate bound, also occur in two distinct pairs, and the spatial arrangement between the individual Fe atoms and the sulfide pairs could be derived from the ^{57}Fe and ^{33}S ENDOR data (*23*). This is illustrated in Fig. 2. Finally, aconitase is able to accommodate a linear 3Fe cluster (Fig. 1) (*25, 26*). This cluster, which had been previously synthesized by Holm's group (*27*), occurs only in a partially unfolded form of aconitase and is not discussed further.

III. Interaction of Cluster and Substrate in the Enzymatic Reaction

Although the aforementioned studies clearly demonstrate the involvement of the iron–sulfur cluster in the enzymatic reaction, the

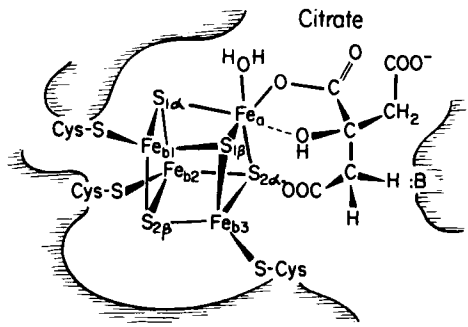

FIG. 2. Representation of ENDOR-derived information about the $[4Fe–4S]^+$ cluster of the aconitase enzyme–substrate complex, showing the two pairs of sulfur ($S_{1\alpha}$ and $S_{1\beta}$; $S_{2\alpha}$ and $S_{2\beta}$) in relationship to the four inequivalent iron sites, Fe_a, Fe_{b1}, Fe_{b2}, and Fe_{b3}, along with the bound substrate. (Reproduced with permission from Ref. *23*. Copyright 1990, American Chemical Society.)

details of this involvement were obtained primarily by ENDOR studies at both X-band (9 GHz) (*28*) and Q-band (35 GHz) (*29, 30*). The feasibility of these studies was established when line broadening was observed in the EPR signal of the $[4Fe–4S]^+$ form of the enzyme in the presence of substrate in ^{17}O-labeled water (*20*). ENDOR measurements were made of enzyme in H_2O, D_2O, and ^{17}O-labeled water in the presence and absence of substrates or inhibitors (*28, 30*). Substrates and inhibitors were in turn specifically labeled with ^2H, ^{13}C, or ^{17}O. The data from these experiments yielded a wealth of information, leading to a detailed picture of the binding of substrate to cluster. The results of ^{17}O ENDOR spectroscopy of substrate labeled individually in each of the carboxyl groups (Table I) indicated binding to the β-carboxyl only (*29*). Similar information was obtained from ^{13}C ENDOR of labeled carboxylates. There was no evidence from these experiments for the binding of hydroxyl from substrate. This led to the interpretation that the predominant species of substrate bound to the $[4Fe–4S]^+$ cluster was *cis*-aconitate in the citrate mode (i.e., through the β-carboxyl). To establish binding in the isocitrate mode (i.e., through the α-carboxyl), the labeled inhibitor nitroisocitrate (1-hydroxy-2-nitro-1,3-propanedicarboxylate) was used. These experiments revealed binding not only to the α-carboxyl but also to the α-hydroxyl (Table I). From this it was concluded that the binding of substrate to cluster involves the formation of a five-membered ring of Fe_a with a carboxyl and hydroxyl of substrate (Fig. 2). This allows for the orientation of either citrate or isocitrate to enzyme such that the proton lost on reaction is in an identical position

TABLE I

ENDOR RESULTS ON ACONITASE WITH ^{17}O-LABELED SUBSTRATES OR ANALOG

Added[a]	^{17}O labeling (●)	Hyperfine coupling constant A_v (MHz)
Citrate	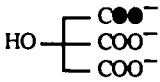	0
Citrate	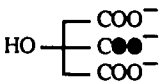	15
Isocitrate	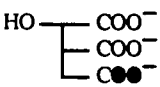	0
Nitroisocitrate	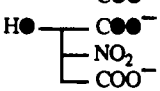	9,13
Nitroisocitrate	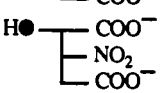	9

[a] Note that in the presence of active aconitase any substrate added is converted to an equilibrium mixture of the three substrates. (Reproduced with permission from Ref. *29*. Copyright 1987.)

for both modes, a requirement established by earlier kinetic and stereochemical studies (*31*, *32*).

In agreement with the X-ray structure, these studies also established that the fourth ligand to Fe_a is not a thiol but rather a hydroxyl from solvent. This is the first documented case in which the fourth ligand to iron in a cluster is not a Cys or Asp residue of the protein. Furthermore, a combination of ^1H, ^2H, and ^{17}O ENDOR demonstrated that this hydroxyl is converted to a water molecule upon the binding of substrate to cluster. These results indicate that Fe_a is six coordinate in the presence of substrate, thus corroborating the earlier conclusions from the MB data.

IV. Crystallographic Structure

The crystal structure of pig heart mitochondrial aconitase was solved and refined at 2.1 Å resolution using data collected aerobically and

crystals grown from ammonium sulfate in the presence of tricarballylate, a weak binding inhibitor (*33*). The structure revealed a [3Fe–4S] cluster and bound sulfate, but no inhibitor, in the active site. Refinement of the structure relied on primary sequence data for pig heart aconitase, 754 residues, 83 kDa (*34*), and partial sequence data for the beef heart enzyme (*35*). The protein structure is arranged into four domains (Fig. 3). The first three from the N terminus are closely associated to create a shallow cavity at the Fe–S cluster and active site. Each of these domains contains a central β sheet with topology common to

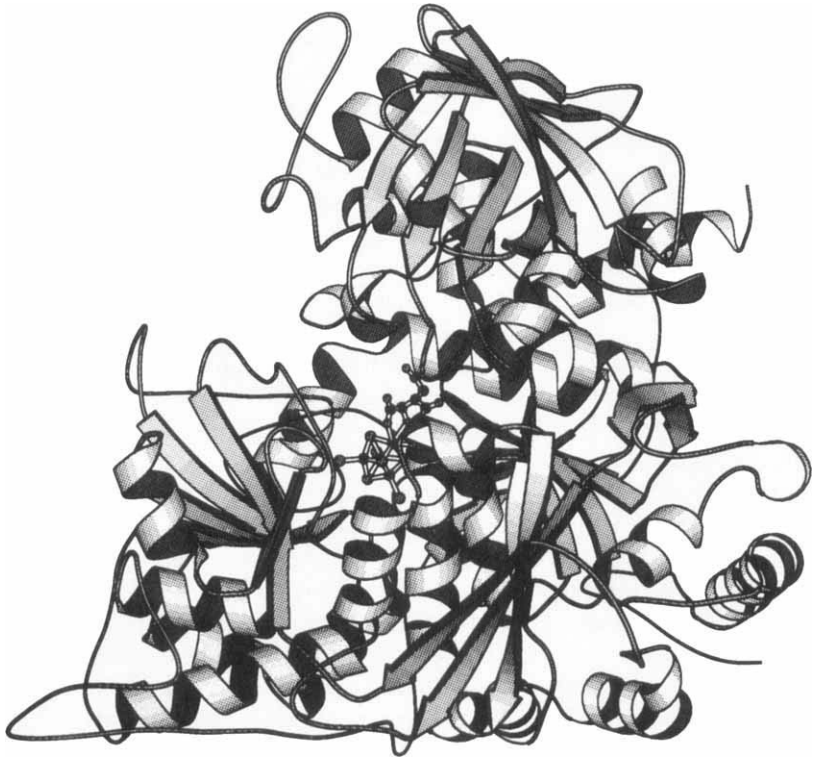

FIG. 3. The structure of heart mitochondrial aconitase showing the polypeptide chain, [4Fe–4S] cluster, and bound isocitrate. Water and three cysteine sulfurs also bonded to the cluster are shown. The protein secondary structure is represented by coils for helices and ribbons for strands within β sheets. The N terminus is at the lower right and the C terminus is at the upper right. In this view the fourth domain is at the top and the three N-terminal domains are arranged from right to left in the lower portion of the molecule. (This image was calculated by G. Gippert at Scripps Research Institute using the program Molscript written by P. Kraulis.)

lactate dehydrogenase. The fourth and largest domain at the C terminus is tethered by an extended polypeptide chain termed the hinge/linker. This creates an extensive cleft running across the molecule between the fourth domain and the first three domains. The Fe–S cluster is at the bottom of this cleft. The fourth domain contains a mixed β sheet of novel topology. Details of the protein structure are described in Ref. *33*.

To assess the [4Fe–4S] form of the enzyme in the crystalline state, the pig heart crystals were soaked anaerobically in ferrous ammonium sulfate and sodium dithionite. The refined structure at 2.5 Å resolution showed that a fourth Fe atom, i.e., Fe_a, was inserted into the [3Fe–4S] cluster isomorphously to create a [4Fe–4S] cluster (*36*). This result confirmed the 3Fe $\rightarrow$ 4Fe conversions observed in aconitase and *D. gigas* Fd II by MB and EPR spectroscopy as discussed above. The ligands of the Fe atoms in the [3Fe–4S] moiety in both the 3Fe and 4Fe forms are three cysteines; however, the ligand of Fe_a is not a cysteine but the oxygen atom from a hydroxyl, as observed in ENDOR experiments (a water molecule was modeled in the crystallographic refinement). Because the [4Fe–4S] cluster was formed by soaking crystals used for the original structure determination, a bound sulfate was again observed in the active site in place of inhibitor.

To obtain crystallographic information about the binding of substrates and inhibitors, pig heart aconitase crystals were used as seeds in anaerobic crystallization experiments in which either pig or beef heart enzyme was incubated in buffers containing the substrate or inhibitor of choice. A new crystal form was obtained that accommodates the binding of several compounds (*37*). (Crystals of the original form used for structure determination invariably cracked when soaked with substrates or tight-binding inhibitors.) Two structures have been reported for aconitase in the new crystal form, both refined at 2.0 Å resolution (*37*). Pig heart enzyme was used for determining the structure with isocitrate bound. The exclusive presence of isocitrate in the crystals was corroborated by MB spectroscopy on a sample consisting of many single crystals. Beef heart enzyme was used for determining the structure with the reaction intermediate analog, nitroisocitrate, bound. The inhibitor binds to the enzyme in a manner virtually identical to that of isocitrate. Both compounds bind to Fe_a of the [4Fe–4S] cluster via a hydroxyl oxygen and one carboxyl oxygen of the α-carboxyl group. A water molecule is also bound, making the Fe six coordinate. Thus, the crystal structures confirm the conclusions drawn from ENDOR experiments regarding the binding mode of isocitrate and nitroisocitrate and the coordination state of Fe_a.

All four domains of aconitase contribute residues to the active site (Fig. 4) (*37*). The residues participate in substrate recognition (Arg 447, Arg 452, Arg 580, Arg 644, Gln 72, Ser 166, and Ser 643), cluster ligation and interaction (Cys 358, Cys 421, Cys 424, Asn 258, and Asn 446), hydrogen bond support of active site side chains (Ala 74, Asp 568, Ser 571, and Thr 567), and catalysis (Ser 642). There are also three histidine–carboxylate pairs: Asp 100–His 101, Asp 165–His 147, and Glu 262–His 167.

The base necessary for proton abstraction from the β-carbon of isocitrate appears to be Ser 642; the oxygen atom is proximal to the calculated hydrogen position and the environment of this oxygen suggests stabilization of an alkoxide (an oxyanion hole formed by the amide and side chain of Arg 644). The histidine–carboxylate pairs appear to be required for proton transfer reactions involving two oxygen atoms bound to Fe_a, one derived from solvent (bound water) and one derived from substrate hydroxyl (Fig. 5). Each of these oxygens is in contact with a histidine and both oxygens through hydrogen bonding are in contact with the side chain of Asp 165, which bridges the two sites on the six-coordinate Fe. The proton transfers are expected to be required for the binding of substrate, as illustrated in Fig. 5, when Fe_a expands

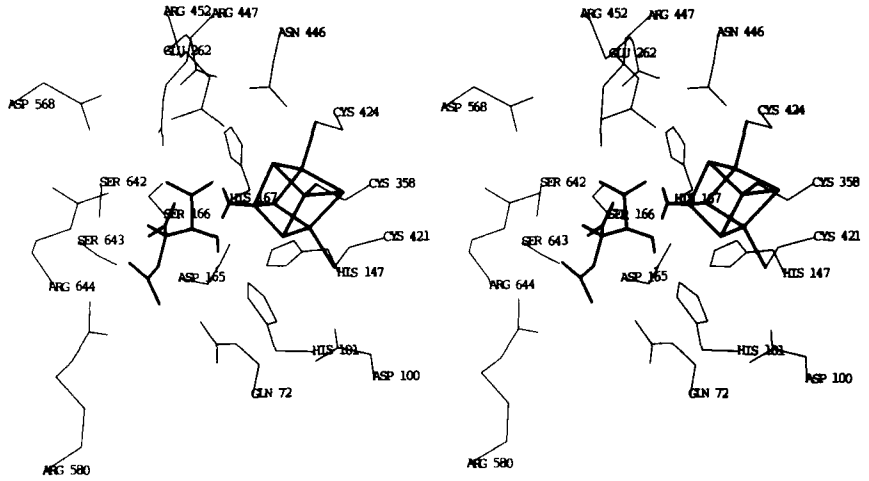

FIG. 4. Stereo view of the active site region in porcine mitochondrial aconitase. The α-carbon atoms and side chains of 19 adjacent residues are shown. The substrate isocitrate is shown in heavy lines along with the [4Fe–4S] cluster and bound H_2O with hydrogens included. (Reproduced with permission from Ref. *37*. Copyright 1991, American Chemical Society.)

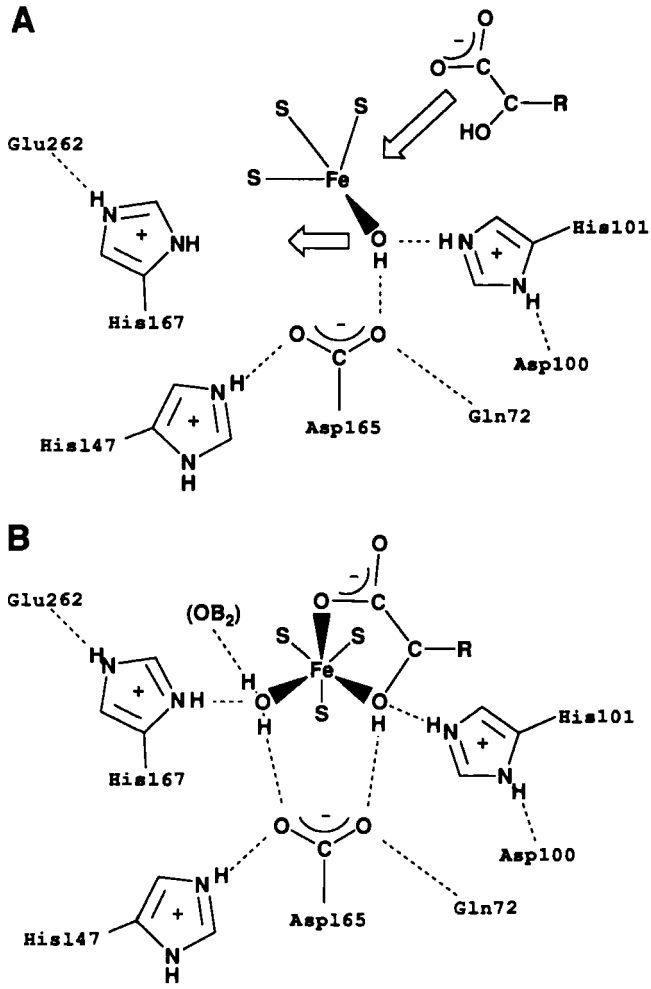

FIG. 5. Schematic representation of the transition from substrate-free aconitase (a) to the substrate-bound form (b). The proton derived from Ser 642 to form an alkoxide is formally equivalent to the proton added to Fe—OH to make Fe—OH_2. The contact of Fe—OH_2 to the β-carboxyl of substrate is shown separately for clarity. All three histidines are assumed to be protonated. (Reproduced with permission from Ref. *37*. Copyright 1991, American Chemical Society.)

its coordination sphere from four to six and Fe–hydroxyl becomes Fe–water as observed by ENDOR (*30*). Further proton transfer involving His 101 is expected to be necessary for cleavage of the C—OH bond in the reaction isocitrate → *cis*-aconitate, as illustrated in Fig. 6.

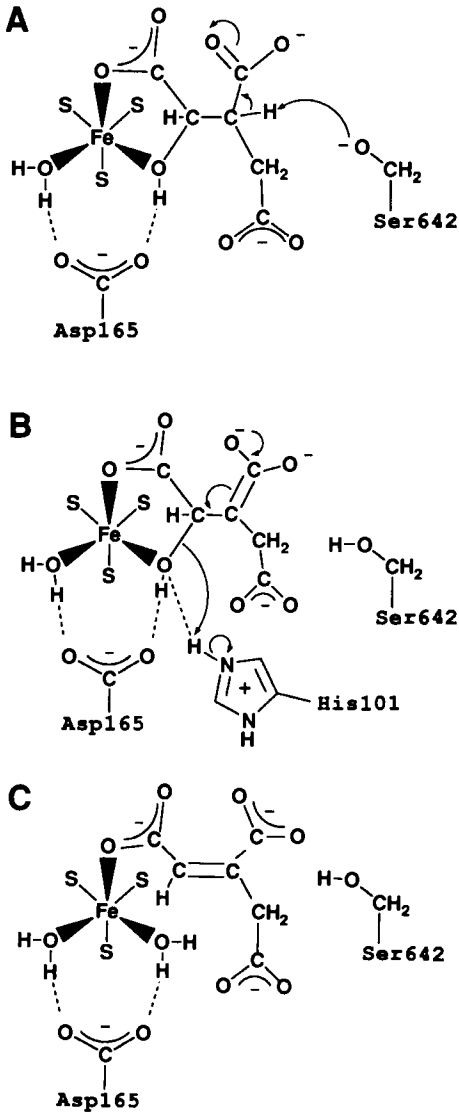

FIG. 6. Schematic representation of the reaction isocitrate → *cis*-aconitate assuming deprotonation of Ser 642 when substrate binds and Fe—OH_2 is formed. Formation of an aci-acid intermediate (A) and collapse of this intermediate (B) forms the product (C). Electron density could also flow from the β-C—H bond to the α-C=C-β double bond, i.e., directly from step A to step C with concomitant cleavage of the α-C—OH bond. (Reproduced with permission from Ref. *37*. Copyright 1991, American Chemical Society.)

Displacement of *cis*-aconitate by another *cis*-aconitate molecule binding to Fe_a via its β-carboxyl (rather than α-carboxyl) (*8*) and reversal of the steps in Fig. 6 would form citrate.

V. Studies on Mutants

With details of the X-ray structure known, and with the availability of the cDNA sequence for pig heart aconitase (*34*), it became possible to study the enzyme by site-directed mutagenesis. Of the 18 active site residues identified by X-ray crystallography, 9 have been individually changed to other amino acids (*38*). The mutations were designed to have a minimum effect on protein structure, and the codons most frequently used by *E. coli* were chosen to achieve high expression. The mutant proteins thus produced have been studied kinetically, examined by EPR, and tested for their ability to form tight complexes with substrate. Native enzyme, when incubated with radiolabeled substrate and rapidly desalted on a gel column anaerobically by centrifugation, will retain bound substrate. Since all the mutants exhibited essentially normal EPR spectra for both the $[3Fe–4S]^+$, $g = 2.02$, and for the $[4Fe–4S]^+$ substrate-free forms, only those changes observed upon addition of substrate to the latter will be discussed. The results of these studies are summarized in Table II.

TABLE II

SUMMARY OF EPR, TIGHT-BINDING, AND KINETIC MEASUREMENTS ON ACONITASE MUTANTS

Mutant	Substrate EPR signal[a]	Tight binding[b]	Relative K_m (isocitrate)[c]	Relative V_{max} isocitrate → aconitate[c]
Beef heart	+	+	1.0	1.0
His 101–Asn	−	−	3–4	1.3×10^{-3}
Asp 165–Ser	−	+	3–4	3×10^{-5}
Arg 452–Gln	±	−	~1	2.1×10^{-3}
Arg 580–Lys	−	−	≥30	1.2×10^{-3}
Ser 642–Ala	+	+	2–3	2.6×10^{-5}
Ser 642–Thr	−	±	1–2	1.7×10^{-4}

[a] (+), Refers to a shift of g values from 2.06, 1.93, and 1.86 to 2.04, 1.85, and 1.78 upon addition of substrate.

[b] (+), Indicates tight binding as described in text.

[c] Ratio of values measured on mutant versus native enzyme under identical conditions. (Adapted from Ref. *38*.)

Of particular interest are the mutants for Ser 642. Before the crystal structure of the enzyme with bound substrate was solved, this residue was not considered a likely candidate for being the base involved in the proton abstraction from substrate. However, analysis of both the Ser 642–Ala and Ser 642–Thr enzymes substantiates the conclusion that this is indeed its function (Figs. 4 and 6). Activity for both of these mutants drops four to five orders of magnitude, depending on substrate. Although according to Bordo and Argos (*39*) both of these substitutions could be considered "safe," there are obvious differences in the EPR and binding properties for these proteins. For the Ser 642–Thr mutant it appears that the added methyl group perturbs the active site such that tight binding and interaction of substrate with cluster, as determined by EPR, are substantially lower than for the alanine mutant.

Another key residue implicated in the catalytic mechanism is Asp 165. Analysis of the X-ray model of enzyme with bound substrate shows that the carboxylate of this amino acid can form hydrogen bonds to both the hydroxyl of substrate as well as to the H_2O ligated to Fe_a (Figs. 5 and 6). Thus this group appears to be essential for the proper orientation of substrate to Fe_a. Analysis of the aspartate-to-serine mutant at this position supports this conclusion. The activity of this enzyme decreases similarly to that of the Ser 642 mutants, and all interactions of substrate with cluster as detected by EPR are abolished. The enzyme, however, still exhibits tight binding.

Arg 580 has been identified as a key binding residue for the γ-carboxyl of substrate (Fig. 4). In keeping with the results deduced from the X-ray structure are results of the examination of the Arg 580–Lys protein. This mutant has a K_m for isocitrate ≥ 30-times that of the wild type and has lost the ability to bind substrate tightly (Table II). The EPR spectrum in the presence of substrate is identical to that of the substrate free form. The increase in K_m may account for the 1000-fold loss of activity for this mutation. The kinetic data also show that the citrate → aconitate and citrate → isocitrate reactions were decreased 10-fold and 100-fold, respectively, when compared to the isocitrate → aconitate reaction. This may suggest that citrate is bound less tightly than isocitrate. Another interesting feature of this mutant is that, in contrast to the native enzyme, it is inhibited by the threo-L_s isomer of isocitrate. Beef or pig heart enzyme give identical activities when assayed with either threo-D_s-isocitrate, the native substrate, or the racemic mixture threo-D_sL_s-isocitrate (*40*). The ratio of the rate of the D_s isomer to the racemic D_sL_s mixture for the Arg 580–Lys enzyme is 2.2. This phenomenon was observed for only two other mutations,

His 147–Asn and Arg 447–Lys, for which the above ratio for the velocities was 13 and 2.7, respectively. Alteration of the active site caused by these mutations obviously allows for the binding of, and subsequent inhibition by, the L_s isomer. The reason for this, particularly in regard to the His 147–Asn mutant, which has over 30% of the activity of the wild type, is unclear at this time.

The only mutant thus far to give an abnormal EPR signal, i.e., a signal not observed with the native enzyme, is Arg 452–Gln in the presence of substrate. Arg 452 is in contact with the α-carboxyl of isocitrate bound to Fe_a (Fig. 4). The K_d for substrate binding to beef heart enzyme as measured by EPR is 1 μM (*19*) whereas the new signal was barely discernible at a substrate : enzyme ratio of 10 : 1. At a ratio of 80 : 1, this new signal, g = 2.02, 1.91, and 1.76, accounted for only 50% of the total. Although tight binding was lost for this mutant, the K_m for isocitrate was essentially normal. The 1000-fold decrease in activity and the abnormal interaction of substrate with the cluster demonstrated by EPR imply that Arg 452 is critical for the proper orientation of the carboxyl bound to Fe_a.

As mentioned previously, His 101 most likely plays a critical role in the loss of substrate hydroxyl by its ability to protonate this group (Figs. 5 and 6B). His 101 is itself within hydrogen bonding distance of Asp 100, thus forming an ion pair with this group (Figs. 4 and 5). The mutant enzymes His 101–Asn and Asp 100–Ser both show a 100-fold decrease in activity and slight increases in their K_m values with isocitrate. They differ, however, in that His 101–Asn shows neither tight binding of substrate nor an EPR signal indicative of substrate bound to the cluster. The opposite is true for Asp 100–Ser. These effects again illustrate the importance of those residues in close proximity to the cluster for properly orienting the substrate with respect to Fe_a and for allowing the necessary interactions to occur for the reaction to proceed at a normal rate. It is interesting to note that all the mutations made thus far, of residues identified as being part of the active site, have significantly altered the catalytic properties of the enzyme.

Although the above discussion has focused on the effects of changes within the protein structure, one should not forget the essential role of the cluster in the function of aconitase. The loss of Fe_a results in an enzyme with 0.3% activity, and to date no other metal replacement has been found that will restore full activity (*41*). However, substitution of Se^{2-} for S^{2-} results in a viable enzyme that not only has activity comparable to the sulfur enzyme but in fact has 1.5 and 2.0 times more activity for the aconitate $\rightarrow$ isocitrate and reverse reactions, respectively (*18*).

VI. Relationship of Cytoplasmic Aconitase to Iron-Responsive Element Binding Protein

Recent developments in the field of iron regulation in cells has focused attention on the cytoplasmic form of aconitase. Although its occurrence has been known for some time, this form of the enzyme has been less well characterized than its mitochondrial counterpart (*42*). The functional significance for its presence in the cytoplasm has never been clearly established. It now appears that cytoplasmic aconitase may be one and the same as the iron-responsive element binding protein (IRE-BP) (*43, 44*), which is expressed ubiquitously in various tissues and species (*45*).

IREs are stem–loop structures (*46*) with a well-defined nucleotide sequence; they were first identified in the mRNAs of ferritin (*47, 48*) and transferrin receptor (*49*). In iron-starved cells, a protein of approximate M_r 90,000 binds to these regulatory elements, and thus affects translation or stability of the mRNA. A computer search was carried out for sequences similar to the sequence for the human liver IRE-BP as determined from its cDNA. This search revealed that there is remarkable homology of this protein with pig heart mitochondrial aconitase (*50, 51*) and yeast isopropyl malate isomerase (*51*). Of the 18 residues identified in the active site of aconitase, all are conserved in the IRE-BP.

Interestingly, IREs have also been found in the mRNA of murine and human δ-aminolevulinic acid synthase (*52, 53*), an enzyme of the heme biosynthetic pathway, and surprisingly in the mRNA of mitochondrial aconitase from pig heart (*53*). Using a partially purified (40%) preparation of beef liver cytoplasmic aconitase, Zheng *et al.* were able to show the binding of this protein to the IRE of mitochondrial aconitase (*44*). This adds to the evidence that cytoplasmic aconitase and IRE-BP are identical (*43*). It also raises the interesting possibility that the synthesis of mitochondrial aconitase is itself regulated by its cytoplasmic counterpart! This new development will undoubtedly attract a whole new audience of researchers, previously working outside the area, to the field of iron–sulfur proteins.

ACKNOWLEDGMENTS

The authors gratefully acknowledge the advice and support of Helmut Beinert in the writing of this article, as well as his contributions to the field in general.

REFERENCES

1. Glusker, J. P., *in* "The Enzymes" (P. D. Boyer, ed.), Vol. 5, pp. 413–439. Academic Press, New York, 1971.
2. Kennedy, C., Rauner, R., and Gawron, O., *Biochem. Biophys. Res. Commun.* **47,** 740 (1972).
3. Emptage, M. H., Kent, T. A., Huynh, B. H., Rawlings, J., Orme-Johnson, W. H., and Münck, E., *J. Biol. Chem.* **255,** 1793 (1980).
4. Kent, T. A., Dreyer, J.-L., Emptage, M. H., Moura, I., Moura, J. J. G., Huynh, B. H., Xavier, A. V., LeGall, J., Beinert, H., Orme-Johnson, W. H., and Münck, E., *in* "Electron Transport and Oxygen Utilization" (C. Ho, ed.), pp. 371–374. Elsevier, New York, 1982.
5. Kent, T. A., Dreyer, J.-L., Kennedy, M. C., Huynh, B. H., Emptage, M. H., Beinert, H., and Münck, E., *Proc. Natl. Acad. Sci. U.S.A.* **79,** 1096 (1982).
6. Kennedy, M. C., Emptage, M. H., Dreyer, J.-L., and Beinert, H., *J. Biol. Chem.* **258,** 11,098 (1983).
7. Beinert, H., and Kennedy, M. C., *Eur. J. Biochem.* **186,** 5 (1989).
8. Emptage, M. H., *in* "Metal Clusters in Proteins" (L. Que, Jr., ed.), ACS Symp. Series 372, pp. 343–371. Am. Chem. Soc., Washington, D.C., 1988.
9. Beinert, H., and Thomson, A. J., *Arch. Biochem. Biophys.* **222,** 333 (1983).
10. Papaefthymiou, V., Girerd, J.-J., Moura, I., Moura, J. J. G., and Münck, E., *J. Am. Chem. Soc.* **109,** 4703 (1987).
11. Noodleman, L., and Baerends, E. J., *J. Am. Chem. Soc.* **106,** 2316 (1984).
12. Münck, E., and Kent, T. A., *Hyperfine Interactions* **27,** 161 (1986).
13. Noodleman, L., and Case, D. A., this volume.
14. Hendrich, M. P., and Debrunner, P. G., *Biophys. J.* **56,** 489 (1989).
15. Beinert, H., Emptage, M. H., Dreyer, J.-L., Scott, R. A., Hahn, J. E., Hodgson, K. O., and Thomson, A. J., *Proc. Natl. Acad. Sci. U.S.A.* **80,** 393 (1983).
16. Kennedy, M. C., and Beinert, H., *J. Biol. Chem.* **263,** 8194 (1988).
17. Kennedy, M. C., Emptage, M. H., and Beinert, H., *J. Biol. Chem.* **259,** 3145 (1984).
18. Surerus, K. K., Kennedy, M. C., Beinert, H., and Münck, E., *Proc. Natl. Acad. Sci. U.S.A.* **86,** 9846 (1989).
19. Emptage, M. H., Dreyer, J.-L., Kennedy, M. C., and Beinert, H., *J. Biol. Chem.* **258,** 11,106 (1983).
20. Emptage, M. H., Kent, T. A., Kennedy, M. C., Beinert, H., and Münck, E., *Proc. Natl. Acad. Sci. U.S.A.* **80,** 4674 (1983).
21. Kent, T. A., Emptage, M. H., Merkle, H., Kennedy, M. C., Beinert, H., and Münck, E., *J. Biol. Chem.* **260,** 6871 (1985).
22. Cammack, R., Dickson, D. P. E., and Johnson, C. E., *in* "Iron Sulfur Proteins" (W. Lovenberg, ed.), Vol. III, pp. 283–330. Academic Press, New York, 1977.
23. Werst, M. M., Kennedy, M. C., Houseman, A. L. P., Beinert, H., and Hoffman, B. M., *Biochemistry* **29,** 10,533 (1990).
24. Middleton, P., Dickson, D. P. E., Johnson, C. E., and Rush, J. D., *Eur. J. Biochem.* **88,** 135 (1978).
25. Kennedy, M. C., Kent, T. A., Emptage, M. H., Merkle, H., Beinert, H., and Münck, E., *J. Biol. Chem.* **259,** 14,463 (1984).
26. Plank, D. W., Kennedy, M. C., Beinert, H., and Howard, J. B., *J. Biol. Chem.* **264,** 20,385 (1989).
27. Hagen, K. S., Watson, A. D., and Holm, R. H., *J. Am. Chem. Soc.* **105,** 3965 (1983).
28. Telser, J., Emptage, M. H., Merkle, H., Kennedy, M. C., Beinert, H., and Hoffman, B. M., *J. Biol. Chem.* **261,** 4840 (1986).

29. Kennedy, M. C., Werst, M., Telser, J., Emptage, M. H., Beinert, H., and Hoffman, B. M., *Proc. Natl. Acad. Sci. U.S.A.* **84,** 8854 (1987).
30. Werst, M. M., Kennedy, M. C., Beinert, H., and Hoffman, B. M. *Biochemistry* **29,** 10,526 (1990).
31. Rose, I. A., and O'Connell, E. L., *J. Biol. Chem.* **242,** 1870 (1967).
32. Gawron, O., Glaid III, A. J., and Fondy, T. P., *J. Am. Chem. Soc.* **80,** 5856 (1958).
33. Robbins, A. H., and Stout, C. D., *Proteins* **5,** 289 (1989).
34. Zheng, L., Andrews, P. C., Hermodson, M. A., Dixon, J. E., and Zalkin, H., *J. Biol. Chem.* **265,** 2814 (1990).
35. Plank, D. W., and Howard, J. B., *J. Biol. Chem.* **263,** 8184 (1988).
36. Robbins, A. H., and Stout, C. D., *Proc. Natl. Acad. Sci. U.S.A.* **86,** 3639 (1989).
37. Lauble, H., Kennedy, M. C., Beinert, H., and Stout, C. D., *Biochemistry* (in press).
38. Zheng, L., Kennedy, M. C., Beinert, H., and Zalkin, H., *J. Biol. Chem.* (in press).
39. Bordo, D., and Argos, P., *J. Mol. Biol.* **217,** 721 (1991).
40. Thomson, J. F., Nance, S. L., Bush, K. J., and Szczepanik, P. A., *Arch. Biochem. Biophys.* **117,** 65 (1966).
41. Villafranca, J. J., and Mildvan, A. S., *J. Biol. Chem.* **246,** 5791 (1971).
42. Dickman, S. R., and Speyer, J. F., *J. Biol. Chem.* **206,** 62 (1954).
43. Kaptain, S., Downey, W. E., Tang, C., Philpott, C., Haile, D., Orloff, D. G., Harford, J. B., Rouault, T. A., and Klausner, R. D., *Proc. Natl. Acad. Sci. U.S.A.* **88,** 10109 (1991).
44. Zheng, L., Kennedy, M. C., Blondin, G. A., Beinert, H., and Zalkin, H., *Mol. Cell. Biol.* (submitted).
45. Neupert, B., Müllner, E. W., Rothenberger, S., Seiser, C., Thompson, N. A., Emery-Goodman, A., and Kühn, L., *J. Inorg. Chem.* **43,** 504 (1991).
46. Leibold, E. A., and Guo, B., *Annu. Rev. Nutr.* **12,** 325 (1992).
47. Hentze, M. W., Rouault, T. A., Caughman, S. W., Dancis, A., Harford, J. B., and Klausner, R. D., *Proc. Natl. Acad. Sci. U.S.A.* **84,** 6730 (1987).
48. Aziz, N., and Munro, H. N., *Proc. Natl. Acad. Sci. U.S.A.* **84,** 8478 (1987).
49. Casey, J. L., Hentze, M. W., Koeller, D. M., Caughman, S. W., Rouault, T. A., Klausner, R. D., and Harford, J. B., *Science* **240,** 924 (1988).
50. Rouault, T. A., Stout, C. D., Kaptain, S., Harford, J. B., and Klausner, R. D., *Cell* **64,** 881 (1991).
51. Hentze, M. W., and Argos, P., *Nucl. Acids Res.* **19,** 1739 (1991).
52. Cox, T. C., Bawden, M. J., Martin, A., and May, B. K., *EMBO J.* **10,** 1891 (1991).
53. Dandekar, T., Stripecke, R., Gray, N. K., Goossen, B., Constable, A., Johansson, H. E., and Hentze, M. W., *EMBO J.* **10,** 1903 (1991).